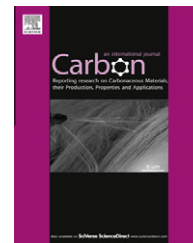


Available at [www.sciencedirect.com](http://www.sciencedirect.com)

SciVerse ScienceDirect

journal homepage: [www.elsevier.com/locate/carbon](http://www.elsevier.com/locate/carbon)

# Synthesis, growth mechanism and thermal stability of copper nanoparticles encapsulated by multi-layer graphene

Shiliang Wang <sup>a,b</sup>, Xiaolin Huang <sup>a</sup>, Yuehui He <sup>a,\*</sup>, Han Huang <sup>a</sup>, Yueqin Wu <sup>b</sup>,  
Lizhen Hou <sup>c</sup>, Xinli Liu <sup>a</sup>, Taimin Yang <sup>a</sup>, Jin Zou <sup>b</sup>, Baiyun Huang <sup>a</sup>

<sup>a</sup> School of Physics Science and Technology, State Key Laboratory for Powder Metallurgy, Central South University, Changsha 410083, China

<sup>b</sup> School of Mechanical and Mining Engineering, Centre for Microscopy and Microanalysis, The University of Queensland, Brisbane, QLD 4072 Australia

<sup>c</sup> Institute of Physics and Information Science, Hunan Normal University, Changsha 410081, China

## ARTICLE INFO

### Article history:

Received 25 August 2011

Accepted 21 December 2011

Available online 12 January 2012

## ABSTRACT

Copper nanoparticles encapsulated by multi-layer graphene have been produced in large quantity (in grams) by metal-organic chemical vapor deposition at 600 °C with copper(II) acetylacetonate powders as precursor. The obtained graphene/copper shell/core nanoparticles were found to be formed by a novel coalescence mechanism that is quite different from the well-known dissolution–precipitation mechanism for some other graphene/metal (such as nickel, iron or cobalt) shell/core nanoparticles. Differential scanning calorimetry and thermogravimetric analyses showed that the copper nanoparticles encapsulated by multi-layer graphene with a thickness of 1–2 nm were thermally stable up to 165 °C in air atmosphere. Moreover, high-resolution transmission electron microscopy showed that the single-crystal copper nanoparticles, after exposure to air for 60 days, did not exhibit any sign of oxidation.

© 2012 Elsevier Ltd. All rights reserved.

## 1. Introduction

Metal nanomaterials have received tremendous scientific and practical interest due to their unique properties and novel applications compared to their bulk counterparts [1–5]. A typical example is the potential applications of metal nanoparticles in ink-jet printing technology. Ink-jet printing technology is considered as a promising alternative to the traditional time-consuming, expensive and environment-unfriendly lithography technology for the fabrication of circuit boards in the electronic industry [6,7]. In this novel technology, conductive inks have now been widely considered as the most critical factor, and the suspensions of metal nanoparticles seem to be the most likely candidates for the preparation of conductive inks [8,9]. Owing to their high conductivity and excellent non-oxidizing properties, noble metal nanoparti-

cles, such as silver and gold, have so far been the most active research objects in the past years [8–10]. However, their high cost prevents them from widespread practical applications. As a result, the synthesis of non-noble metal nanoparticles with decent thermal stability and oxidation resistivity has now become of great interest from a scientific and industrial point of view.

Copper (Cu) nanoparticles, due to their relatively low cost and high electrical conductivity, exhibit high potential for replacing the noble metal nanoparticles used in conductive inks [11,12]. However, bare Cu nanoparticles exposed to air at room temperature will be oxidized to form Cu<sub>2</sub>O within several hours [13,14]. Therefore, the problem of their poor oxidation resistance must be resolved before they can be applied into practice. Recently, Cu nanoparticles encapsulated by carbon (C) shells, i.e., C/Cu shell/core nanoparticles, have

\* Corresponding author: Fax: +86 731 88836144.

E-mail address: [yuehui@mail.csu.edu.cn](mailto:yuehui@mail.csu.edu.cn) (Y. He).

0008-6223/\$ - see front matter © 2012 Elsevier Ltd. All rights reserved.

doi:10.1016/j.carbon.2011.12.063

attracted intense interest, because the C shells can serve as the shields to protect the Cu nanocores from oxidation [15–21]. Nevertheless, as these C shells are usually amorphous and/or too thick, their conductivity is typically quite poor [20]. As a result, these C/Cu nanoparticles are not suitable for producing conductive inks.

It is well-known that multi-layer graphene has high conductivity [22] and can be used as excellent conducting electrodes [23,24]. Therefore, a shell of multi-layer graphene can serve as the dual role of protecting the metal nanocore from oxidation [25–27] and conductively connecting the neighbor metal nanocores [28]. This suggests that Cu nanoparticles encapsulated by multi-layer graphene, i.e. graphene/Cu shell/core nanoparticles, should be an ideal material for fabricating conductive inks. For example, Luechinger et al. have successfully fabricated ink-printed electrical circuits using self-manufactured copper/carbon particles [29]. However, the graphene formed on the surface of Cu is usually single-layer, rather than multi-layer, because its formation process is based on the adsorption–diffusion mechanism instead of the dissolution–precipitation mechanism [30]. According to the adsorption–diffusion mechanism, the pre-formed single-layer C atoms can passivate the Cu surface, and dramatically hinder the formation of multi-layer graphene on Cu [30,31]. Furthermore, the growth temperature of graphene on Cu is typically about 1000 °C, which has been above the melting point of Cu nanoparticles [32]. Therefore, it has been very challenging to synthesize graphene/Cu shell/core nanoparticles.

In this paper, we report the large-scale fabrication of Cu nanoparticles encapsulated by multi-layer graphene by using a one-step metal-organic CVD at 600 °C. A novel coalescence mechanism was proposed to explain the formation of the graphene/Cu shell/core nanoparticles at the relatively low temperature. Both differential scanning calorimetry and thermogravimetric (DSC–TG) and high-resolution transmission electron microscopy (HRTEM) analyses showed that the graphene/Cu shell/core nanoparticles exhibited excellent thermal stability.

## 2. Experimental

The graphene-encapsulated Cu nanoparticles were synthesized in a horizontal tube furnace with a vacuum pump system, as shown in Fig. 1. Analytical copper(II) acetylacetonate ( $\text{Cu}(\text{acac})_2$ , Aldrich Chemical Co., 97%) powder was loaded

into a quartz boat installed in the evaporating region with a temperature of 150 °C (upstream) in the furnace. The gaseous  $\text{Cu}(\text{acac})_2$ , formed in the evaporating region, was then transported to the reaction region of 600 °C (midstream) by the carrier gas  $\text{H}_2$  (flow: 200 standard cubic centimeters per minute; pressure: 50 Pa). The resultant nanoparticles were then deposited on/in the stainless-steel wool located at the deposition region (downstream). In addition, two parallel experiments were carried out by changing the temperature of the reaction region to 500 and 700 °C, respectively, in order to investigate the effects of the reaction temperature on the formation of nanoparticles.

The synthesized nanoparticles were analyzed by X-ray diffraction (XRD, Rigaku D max 2500 VB), Raman Spectrometer (LabRAM HR 800), field emission scanning electron microscopy (FE-SEM; FEI Nova NanoSEM 230) and transmission electron microscopy (TEM; FEI Tecnai F30 and F20 operated at 200 kV). The thermal stability of the nanoparticles was tested in a flowing air atmosphere at a heating rate of 10 °C/min in a thermogravimetric differential analyzer (Model Netzsch Sta 449C, Germany). The samples, after exposure to the air for 60 days at ambient condition, were re-examined by HRTEM to observe the possible morphological and structural changes due to oxidation. In addition, the samples were re-examined by XRD to check whether there is a fraction of nanoparticles that was oxidized during this period of air exposure.

## 3. Results and discussion

### 3.1. Morphological and structural characteristics of the graphene/Cu shell/core nanoparticles

The stainless-steel wool, after taken out from the furnace tube, was found to be fully covered with black powder. Typically, several grams of this black powder could be produced in one test run. Fig. 2a presents the typical SEM image of the black powder synthesized at 600 °C, showing that the powder consists of nanosized particles. The inset in Fig. 2a shows the optical photo of the powder in black after shaken off from the stainless-steel wool. High-magnification SEM imaging (Fig. 2b) further reveals that these nanoparticles have a uniform diameter of about 20 nm. Fig. 3a is the XRD diffractograms of the resultant nanoparticles (the black line) and the commercial Cu powder with an average diameter of 75  $\mu\text{m}$  (the red line). Three diffraction peaks with high

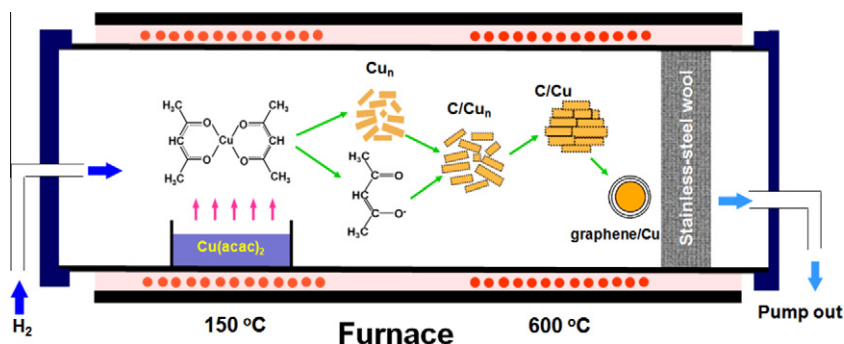
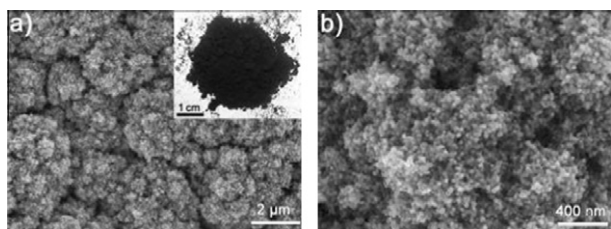


Fig. 1 – Schematic of the experimental setup and the growth model for the graphene/Cu shell/core nanoparticles.



**Fig. 2 – (a) Low-magnification and (b) high-magnification SEM images of the nanoparticles obtained at 600 °C. Inset in (a) shows the optical image of the nanoparticles shaken off from the steel wool.**

intensity located at 43.20°, 50.30° and 73.96° correspond to the three crystalline planes of (111), (200) and (220) of the face centered cubic (fcc) Cu (JCPDS 4-836,  $a = 0.3615$  nm), respectively. The obviously broadened diffraction peaks suggest that the resultant nanoparticles should have a very small crystallite size. An average crystallite size of about 17 nm for the Cu nanoparticles was calculated by using the Scherrer's relation. In the Raman spectrum of these nanoparticles (Fig. 3b), the first-order region of the Raman spectrum of the nanoparticles shows a G band at 1588  $\text{cm}^{-1}$  and a D band at 1347  $\text{cm}^{-1}$ . The G band originates from the stretching motion of  $\text{sp}^2$  carbon pairs in both rings and chains [33], while the D band arises from defects in the hexagonal  $\text{sp}^2$  carbon network or the finite particle-size effect [33,34]. In addition to the first-order bands, several combination bands located at 2694, 2937 and 3150  $\text{cm}^{-1}$  can also be observed in the Raman spectra. These bands are consistent with those of the non-planar graphene, and can be assigned to 2D, D + G and 2D, respectively [35].

The morphological and structural characteristics of the nanoparticles formed at 600 °C were further characterized using TEM. TEM images and the corresponding selected-area electron diffraction (SAED) pattern, shown in Fig. 4a and b, revealed that most of the synthesized nanoparticles are spherical single-crystal Cu particles completely encapsulated by multi-layer graphene with a thickness of 1–2 nm. In addition, a quite small quantity of Cu nanoparticles, composed of two hemispheres with high contrast, can also be observed by TEM (as indicated by the arrows in Fig. 4a). HRTEM analysis (Fig. 4c) revealed that these nanoparticles were {111} twin crystals that usually appearing in fcc crystals [36]. During

the TEM examination, we have measured more than 400 nanoparticles and found that the diameters of the particles varied from 6 to 40 nm (Fig. 4d), leading to an average diameter of 21 nm for the shell/core nanoparticles and a thickness of 1–2 nm for the graphene shells. Therefore, the average diameter of the Cu cores, 18 nm, obtained directly TEM agrees well with the calculated value of 17 nm using the Scherrer's equation.

Fig. 5 shows the TEM results of the nanoparticles formed in the parallel experiments with different reaction temperatures. It can be found that the nanoparticles generated at 500 °C also have a shell/core nanostructure (see Fig. 5a and b). However, the surface contours of these nanoparticles appear to be rougher than those fabricated at 600 °C, and it is quite common to see that an individual nanoparticle consists of several regions with different contrast. HRTEM analysis further revealed that these regions with different contrast corresponded to the nanocrystallites with different orientations (Fig. 5b). TEM images also revealed that the spherical nanoparticles fabricated at 700 °C have relatively thick carbon shells of  $\sim 10$  nm (Fig. 5c). Fig. 5d is a typical HRTEM image of an individual nanoparticle, showing that it has a single-crystalline Cu nanocore, a graphene-like inner shell, and an amorphous outer carbon shell. These results strongly suggest that the Cu nanocores should be likely formed by the coalescence of smaller nanocrystallites, and the high temperature should favor the coalescence of the nanocrystallites [37].

### 3.2. Formation mechanism of the graphene/Cu shell/core nanoparticles

It is well-documented that at a suitable temperature the C atoms can continually dissolve into and then precipitate from Ni, Fe or Co nanoparticles to form carbon filaments [38], multi-wall carbon nanotubes [39], or multi-layer graphene [40]. However, the quite low solubility of C in Cu could limit the process of dissolution–precipitation of C atoms in Cu, and the C atoms usually adsorb onto and then move along the Cu surface, and finally lead to the growth of single-wall carbon nanotubes [41] or single-layer graphene [42]. Moreover, it has been well-demonstrated that the single-layer C atoms can passivate the Cu surface, and dramatically hinder the formation of

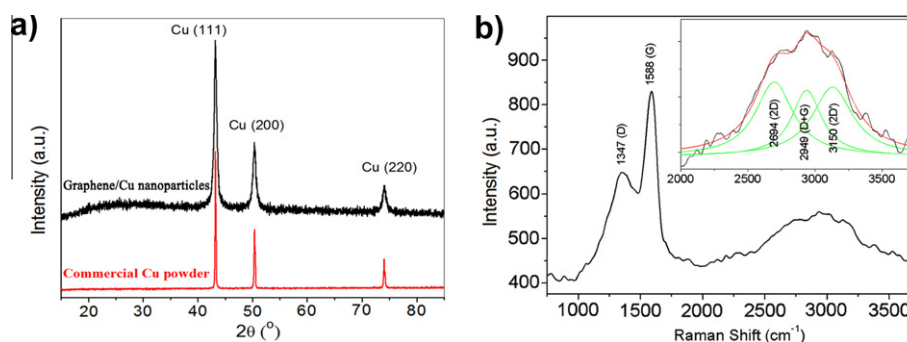


**Fig. 3 – (a) XRD diffractograms of the synthesized nanoparticles (the up black line) and the commercial copper powder with an average diameter of 75  $\mu\text{m}$  (the below red line). (b) Raman spectrum of the synthesized nanoparticles. (For interpretation of the references to color in this figure legend, the reader is referred to the web version of this article.)**

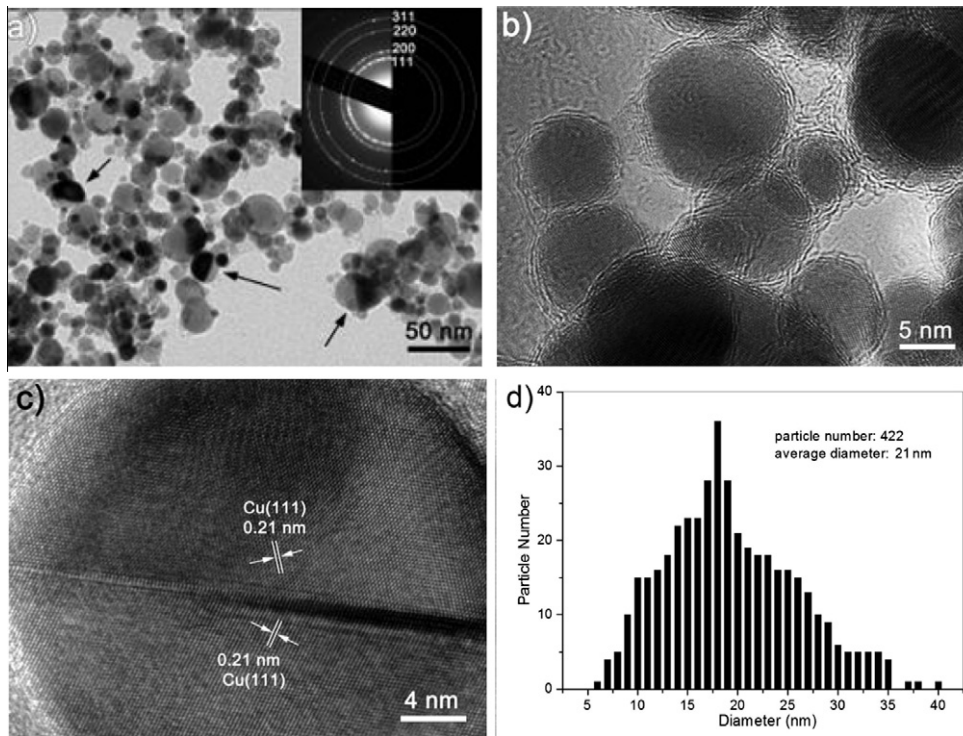


**Fig. 4** – (a) Low-magnification TEM image and the corresponding SAED pattern of the synthesized nanoparticles. (b) HRTEM image of the synthesized Cu nanoparticles encapsulated by multi-layer graphene. (c) HRTEM image of the {1 1 1} twinning within a single Cu core. (d) Particle-size distribution of the synthesized nanoparticles.

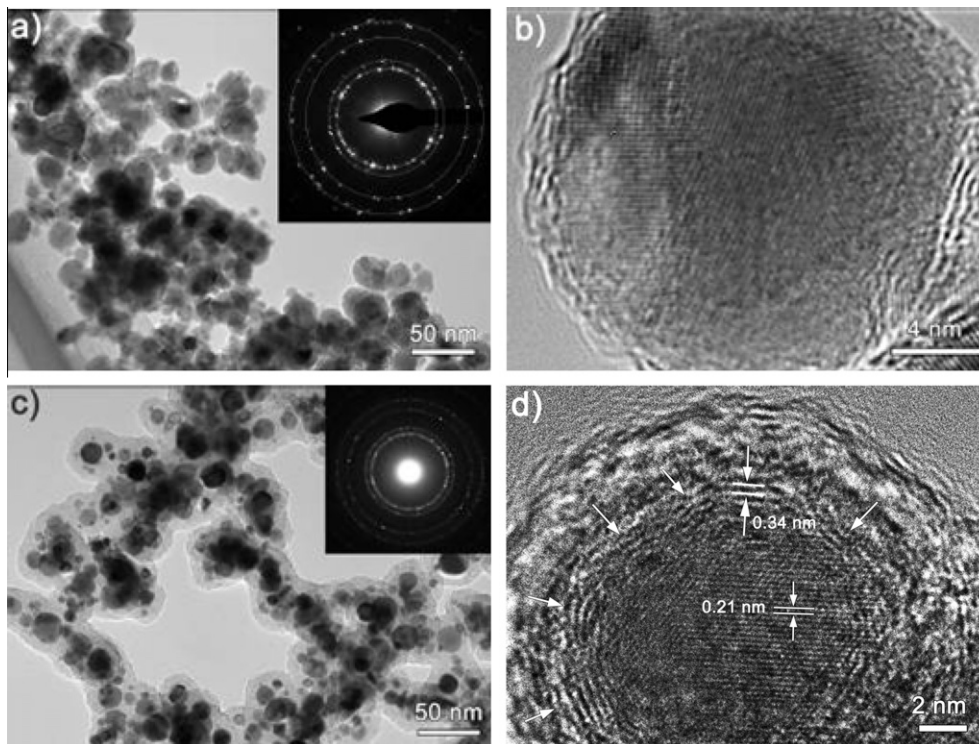
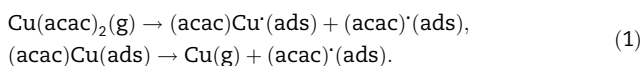


**Fig. 5** – (a) Low-magnification TEM image and SEAD pattern of the nanoparticles obtained at 500 °C. (b) HRTEM image of the nanocrystallites within a single nanoparticle. (c) Low-magnification TEM image and SEAD pattern of the nanoparticles obtained at 700 °C. (d) HRTEM image of a single nanoparticle with a Cu core, an inner graphene shell and an outer amorphous carbon shell.

multi-layer graphene on Cu [30]. Therefore, a new mechanism must be proposed to explain the formation of multi-layer graphene on Cu nanoparticles in our experiments.

Here, we propose a novel coalescence model to explain the formation of the graphene/Cu shell/core nanoparticles, which includes four stages: (1) formation and transport of gaseous  $\text{Cu}(\text{acac})_2$ , (2) decomposition of  $\text{Cu}(\text{acac})_2$  and formation of small C/Cu nanoclusters, (3) formation of C/Cu nanoagglomerates and (4) formation of the graphene/Cu shell/core nanoparticles (also see Fig. 1). In the first stage,  $\text{Cu}(\text{acac})_2$  evaporates at the evaporating region of 150 °C and then transport to the reaction region of 600 °C by the carrier gas  $\text{H}_2$ . Previous studies have demonstrated that  $\text{Cu}(\text{acac})_2$  possesses a relatively high vapor pressure at temperatures over 100 °C (e.g., ~40 Pa at 150 °C) and decomposes at temperatures over 190 °C in  $\text{H}_2$  [42,43]. In the second stage, gaseous  $\text{Cu}(\text{acac})_2$  in  $\text{H}_2$  is decomposed, which involves a radical mechanism [42,43], as expressed by the following reactions:



The resulting Cu vapor then condenses to form stable copper nanoclusters,  $\text{Cu}_n$ , with  $n \leq 13$  [44,45]. The generated  $\text{Cu}_n$  nanoclusters, floating in the reaction atmosphere, act as the catalysts to accelerate the decomposition of the acetyl-acetone radical,  $(\text{acac})'$  [43]. The resultant C atoms are then expected to be adsorbed on the  $\text{Cu}_n$  surface and thus form the C/ $\text{Cu}_n$  nanoclusters [30,31]. In the third stage, the C/ $\text{Cu}_n$  nanoclusters aggregate together to form larger C/Cu nanoagglomerates during the collision process in the reaction atmosphere, due to their high surface activity and high surface adsorption [46]. In the final stage, the Cu atoms within an individual C/Cu nanoagglomerates coalesces into a Cu nanocore, while the carbon atoms diffuse out onto the surface and form a graphene shell, due to the rapid interdiffusion of Cu and C atoms at the given temperatures and the quite low solubility of C in Cu [47].

Obviously, the coalescence mechanism is somehow different from those involved in the dissolution and the subsequent precipitation process of C atoms in Ni, Fe or Co, to form the corresponding graphene/metal shell/core nanoparticles [38]. As the coalescence of Cu nanoclusters need extra energy [37], the high reaction temperature will favor the coalescence process. This is why the Cu cores formed at high temperatures have much less or no defects (Figs. 4b and 5d). In addition, as a high reaction temperature can also lead to a more rapid non-catalytic decomposition of acetyl-acetone radical [42,43]; the resulting C atoms then deposit or adsorb on the surfaces of the pre-formed graphene/Cu shell/core nanoparticles. These additive carbon atoms will form the amorphous shells on the pre-formed graphene shells (Fig. 5d), because the graphitization temperature of the deposited carbon films is far higher than 700 °C used in our experiments [34].

### 3.3. Thermal stability of the graphene/Cu shell/core nanoparticles

The thermal stability of the graphene/Cu shell/core nanoparticles was measured by a thermogravimetric differential analyzer. As shown in Fig. 6a, the TG curve shows that after

a slight weight loss of 0.8% at the initial stage due to the evaporation of the physisorbed water [29,48], the nanoparticles gain a weight raise of 10.2% at 234 °C. After a weight loss of 1.3% at 262 °C and a weight gain of 1.6% at 296 °C, the nanoparticles finally hold with a total weight ratio of 10.0% at about 400 °C. The DSC curve indicates that the nanoparticles have the first exothermic peak at 215 °C that begins at 165 °C, and the second higher exothermic peak at 255 °C that begins at 234 °C. The DSC–TG results clearly suggest that the

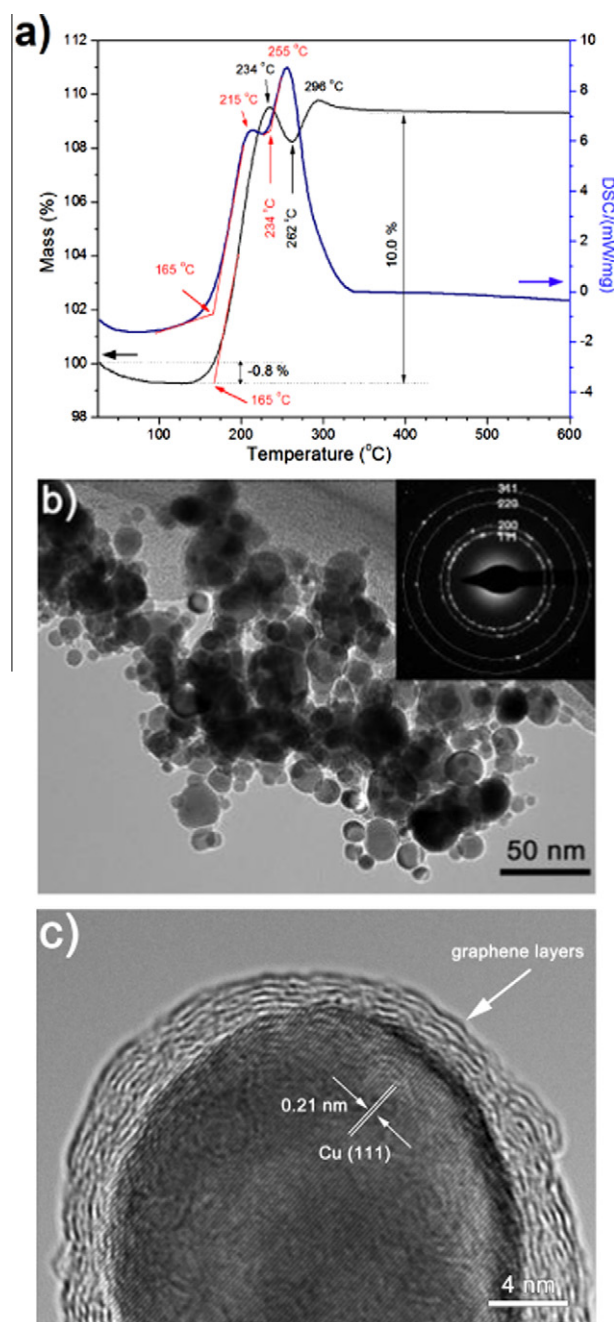


**Fig. 6 – (a)** DSC–TG curve of the graphene/Cu shell/core nanoparticles. **(b)** TEM image and SEAD pattern of the graphene/Cu shell/core nanoparticles after exposure to air for 60 days. **(c)** Typical HRTEM image of a graphene/Cu shell/core nanoparticle shown in (b).

oxidation of Cu nanocores by the reaction, i.e.  $\text{Cu(s)} \rightarrow \text{Cu}_2\text{O(s)}$ , should commence at about 165 °C and finish at about 230 °C, which results in a weight gain of 10.2% (theoretically 11.1%). The further oxidation of cuprous oxide,  $\text{Cu}_2\text{O(s)} \rightarrow \text{CuO(s)}$ , and the oxidation of the graphene shells,  $\text{C(s)} \rightarrow \text{CO}_2\text{(g)}$ , begin at about 234 °C. The oxidation process may result in a slight weight loss at 262 °C and a subsequently slight weight gain at 296 °C, due to the rapid combustion of the graphene shells at about 255 °C and the relatively slow oxidation rate of  $\text{Cu}_2\text{O}$ . The total mass gain of 10.0% of the nanoparticles during the oxidation process suggests that the weight content of the graphene shells in the nanoparticles should be approximately 12.1%, based on the assumption that all Cu has transferred to CuO and all C has been burnt out. Using the average particle diameter of 21 nm and the density of 2.3 g/cm<sup>3</sup> for graphite and 8.9 g/cm<sup>3</sup> for Cu, the thickness of the graphene shell is calculated to be 1.7 nm, which agrees well with the TEM measurement.

The excellent oxidation resistance of the graphene/Cu shell/core nanoparticles can also be characterized by direct TEM observation and XRD examination. Fig. 6b represents the TEM image and the corresponding SAED pattern of the nanoparticles after exposure to air atmosphere at room temperature for 60 days. No visible evidence of  $\text{Cu}_2\text{O}$  or CuO, and morphological changes can be detected from these shell/core nanoparticles. Fig. 6c shows a typical HRTEM image of a nanoparticle, showing that under the protection of the graphene shell with a thickness of 2 nm, the Cu nanocore with a diameter of 20 nm still has a perfect single-crystalline structure. These results directly demonstrate that the graphene shells can effectively protect the Cu nanocores from oxidation. In addition, to check the oxidation resistance of the whole sample, we re-checked the nanoparticles exposure to air under ambient conditions for more than two months, and obtained the identical XRD diffractogram (not shown here) as that showed in Fig. 3a. This result further revealed that the copper nanoparticles encapsulated by multi-layer graphene, on a whole, are also stable against oxidation at least at X-ray detection level.

#### 4. Conclusions

We have developed a low-cost, high-yield and one-step metal-organic CVD to fabricate Cu nanoparticles encapsulated by multi-layer graphene at 600 °C. The synthesized graphene/Cu shell/core nanoparticles have single-crystalline Cu nanocores with an average diameter of 18 nm and multi-layer graphene shells with a thickness of 1–2 nm. The obtained shell/core nanoparticles were formed by the coalescence of Cu and C atoms within the C/Cu nanoagglomerates, which originated from the agglomeration of C/Cu nanoclusters suspended in the reaction atmosphere during a collision process. The graphene/Cu shell/core nanoparticles demonstrated excellent oxidation resistance, and have high potential for replacing the expensive noble metal nanoparticles utilized in the conductive inks.

#### Acknowledgements

This study is supported by the National Natural Science Foundation of China (Grant Nos. 50825102, 50804057, 51074188, 51071178, 50721003, and 50823006) and the Postdoctoral Science Foundation of Central South University.

#### REFERENCES

- [1] Keating CD, Natan MJ. Striped metal nanowires as building blocks and optical tags. *Adv Mater* 2003;15(5):451–4.
- [2] Wang SL, He YH, Fang XS, Zou J, Wang Y, Huang H, et al. Structure and field-emission properties of sub-micrometer-sized tungsten-whisker arrays fabricated by vapor deposition. *Adv Mater* 2009;21(23):2387–92.
- [3] Murphy CJ, Sau TK, Gole AM, Orendorff CJ, Gao J, Gou L, et al. Anisotropic metal nanoparticles: synthesis, assembly, and optical applications. *J Phys Chem B* 2005;109(29):13857–70.
- [4] Huang H, Wu YQ, Wang SL, He YH, Zou J, Huang BY, et al. Mechanical properties of single crystal tungsten microwhiskers characterized by nanoindentation. *Mater Sci Eng, A* 2009;53(1-2):193–8.
- [5] Wang SL, He YH, Zou J, Wang Y, Huang H, Huang BY, et al. Catalytic growth of metallic tungsten whiskers based on the vapor–solid–solid mechanism. *Nanotechnology* 2008;19(34):345604. 5pp.
- [6] de Gans BJ, Duineveld PC, Schubert US. Inkjet printing of polymers: state of the art and future developments. *Adv Mater* 2004;16(3):203–13.
- [7] Street RA, Wong WS, Ready SE, Chabinyc ML, Arias AC, Limb S, et al. Jet printing flexible displays. *Mater Today* 2006;9(4):32–7.
- [8] Magdassi S, Bassa A, Vinetsky Y, Kamyshny A. Silver nanoparticles as pigments for water-based ink-jet inks. *Chem Mater* 2003;15(11):2208–17.
- [9] van Osch THJ, Perelaer J, de Laat AWM, Schubert US. Inkjet printing of narrow conductive tracks on untreated polymeric substrates. *Adv Mater* 2008;20(2):343–5.
- [10] Anto BT, Sivaramakrishnan S, Chua L-L, Ho PKH. Hydrophilic sparse ionic monolayer-protected metal nanoparticles: highly concentrated nano-Au and Nano-Ag “Inks” that can be sintered to near-bulk conductivity at 150 °C. *Adv Funct Mater* 2010;20(2):296–303.
- [11] Park BK, Kim D, Jeong S, Moon J, Kim JS. Direct writing of copper conductive patterns by ink-jet printing. *Thin Solid Films* 2007;515(19):7706–11.
- [12] Jang S, Seo Y, Choi J, Kim T, Cho J, Kim S, et al. Sintering of inkjet printed copper nanoparticles for flexible electronics. *Scr Mater* 2010;62(5):258–61.
- [13] Liu XM, Zhou YC. Electrochemical synthesis and room temperature oxidation behavior of Cu nanowires. *J Mater Res* 2005;20(9):2371–8.
- [14] Chen CH, Yamaguchi T, Sugawara KI, Koga K. Role of stress in the self-limiting oxidation of copper nanoparticles. *J Phys Chem B* 2005;109(44):20669–72.
- [15] Bokhonov B, Novopashin S. In situ investigation of morphological and phase changes during thermal annealing and oxidation of carbon-encapsulated copper nanoparticles. *J Nanopart Res* 2010;12:2771–7.
- [16] Hao C, Xiao F, Cui Z. Preparation and structure of carbon encapsulated copper nanoparticles. *J Nanopart Res* 2008;10(1):47–51.

- [17] Jacob DS, Genish I, Klein L, Gedanken A. Carbon-coated core shell structured copper and nickel nanoparticles synthesized in an ionic liquid. *J Phys Chem B* 2006;110(36):17711–4.
- [18] Li H, Kang W, Xi B, Yan Y, Bi H, Zhu Y, et al. Thermal synthesis of Cu@carbon spherical core-shell structures from carbonaceous matrices containing embedded copper particles. *Carbon* 2010;48(2):464–9.
- [19] Li J, Liu C-y. Carbon-coated copper nanoparticles: synthesis, characterization and optical properties. *New J Chem* 2009;33(7):1474–7.
- [20] Gao MR, Xu WH, Luo LB, Zhan YJ, Yu SH. Coaxial metal nano-/microcables with isolating sheath: synthetic methodology and their application as interconnects. *Adv Mater* 2010;22(17):1977–81.
- [21] Wang S, He Y, Liu X, Huang H, Zou J, Song M, et al. Novel C/Cu sheath/core nanostructures synthesized via low-temperature MOCVD. *Nanotechnology* 2011;22(40):405704. 7pp.
- [22] Reina A, Jia XT, Ho J, Nezich D, Son HB, Bulovic V, et al. Large area, few-layer graphene films on arbitrary substrates by chemical vapor deposition. *Nano Lett* 2009;9(1):30–5.
- [23] Kim KS, Zhao Y, Jang H, Lee SY, Kim JM, Kim KS, et al. Large-scale pattern growth of graphene films for stretchable transparent electrodes. *Nature* 2009;457(7230):706–10.
- [24] Jo G, Choe M, Cho CY, Kim JH, Park W, Lee S, et al. Large-scale patterned multi-layer graphene films as transparent conducting electrodes for GaN light-emitting diodes. *Nanotechnology* 2010;21(17):175201. 6pp.
- [25] Hayashi T, Hirano S, Tomita M, Umemura S. Magnetic thin films of cobalt nanocrystals encapsulated in graphite-like carbon. *Nature* 1996;381(6585):772–4.
- [26] Athanassiou EK, Grass RN, Stark WJ. Large-scale production of carbon-coated copper nanoparticles for sensor applications. *Nanotechnology* 2006;17(6):1668–73.
- [27] Seo WS, Lee JH, Sun XM, Suzuki Y, Mann D, Liu Z, et al. FeCo/graphitic-shell nanocrystals as advanced magnetic-resonance-imaging and near-infrared agents. *Nat Mater* 2006;5(12):971–6.
- [28] Stankovich S, Dikin DA, Dommett GHB, Kohlhaas KM, Zimney EJ, Stach EA, et al. Graphene-based composite materials. *Nature* 2006;442(7100):282–6.
- [29] Luechinger NA, Athanassiou EK, Stark WJ. Graphene-stabilized copper nanoparticles as an air-stable substitute for silver and gold in low-cost ink-jet printable electronics. *Nanotechnology* 2008;19(44):445201. 6pp.
- [30] Li XS, Cai WW, Colombo L, Ruoff RS. Evolution of graphene growth on Ni and Cu by carbon isotope labeling. *Nano Lett* 2009;9(12):4268–72.
- [31] Li X, Cai W, An J, Kim S, Nah J, Yang D, et al. Large-area synthesis of high-quality and uniform graphene films on copper foils. *Science* 2009;324(5932):1312–4.
- [32] Mattevi C, Kim H, Chhowalla M. A review of chemical vapour deposition of graphene on copper. *J Mater Chem* 2011;21(10):3324–34.
- [33] Ferrari AC, Robertson J. Resonant raman spectroscopy of disordered, amorphous, and diamond like carbon. *Phys Rev B* 2001;64(7):075414.
- [34] Pimenta MA, Dresselhaus G, Dresselhaus MS, Cancado LG, Jorio A, Saito R. Studying disorder in graphite-based systems by Raman spectroscopy. *Phys Chem Chem Phys* 2007;9(11):1276–90.
- [35] Tan P, Dimovski S, Gogotsi Y. Raman scattering of non-planar graphite: arched edges, polyhedral crystals, whiskers and cones. *Philos Trans R Soc London, Ser A: Math, Phys Eng Sci* 2004;362(1824):2289–310.
- [36] Kelly A, Groves GW, Kidd P. *Crystallography and crystal defects*. Brisbane: John Wiley & Sons Ltd.; 2000.
- [37] Zhang J, Huang F, Lin Z. Progress of nanocrystalline growth kinetics based on oriented attachment. *Nanoscale* 2010;2(1):18–34.
- [38] Baker RTK. Catalytic growth of carbon filaments. *Carbon* 1989;27(3):315–23.
- [39] Charlier J-C, Iijima S. Growth mechanisms of carbon nanotubes. In: Dresselhaus M, Dresselhaus G, Avouris P, editors. *Carbon nanotubes*. Berlin/Heidelberg: Springer; 2001. p. 55–81.
- [40] Nolan PE, Lynch DC, Cutler AH. Catalytic disproportionation of CO in the absence of hydrogen: encapsulating shell carbon formation. *Carbon* 1994;32(3):477–83.
- [41] Zhou W, Han Z, Wang J, Zhang Y, Jin Z, Sun X, et al. Copper catalyzing growth of single-walled carbon nanotubes on substrates. *Nano Lett* 2006;6(12):2987–90.
- [42] Pauleau Y, Fasasi AY. Kinetics of sublimation of copper(II) acetylacetonate complex used for chemical vapor deposition of copper films. *Chem Mater* 1991;3(1):45–50.
- [43] Vertoprakhov VN, Krupoder SA. Preparation of thin copper films from the vapour phase of volatile copper(I) and copper(II) derivatives by the CVD method. *Russ Chem Rev* 2000;69(12):1057–82.
- [44] Vilar-Vidal N, Blanco MC, López-Quintela MA, Rivas J, Serra C. Electrochemical synthesis of very stable photoluminescent copper clusters. *J Phys Chem C* 2010;114(38):15924–30.
- [45] Wei W, Lu Y, Chen W, Chen S. One-pot synthesis, photoluminescence, and electrocatalytic properties of subnanometer-sized copper clusters. *J Am Chem Soc* 2011;133(7):2060–3.
- [46] Ayyappan S, Gopalan RS, Subbanna GN, Rao CNR. Nanoparticles of Ag, Au, Pd, and Cu produced by alcohol reduction of the salts. *J Mater Res* 1997;12(2):398–401.
- [47] López GA, Mittemeijer EJ. The solubility of C in solid Cu. *Scr Mater* 2004;51(1):1–5.
- [48] Ponder SM, Darab JG, Bucher J, Caulder D, Craig I, Davis L, et al. Surface chemistry and electrochemistry of supported zerovalent iron nanoparticles in the remediation of aqueous metal contaminants. *Chem Mater* 2001;13(2):479–86.